The original publication is available at https://doi.org/10.1007/s11270-022-05921-1

Algal organic matter degradation by chemical and photo-chemical processes: a comparative study

Luan de Souza Leite[1], Kamila Jessie Sammarro Silva[1], Danilo Vitorino dos Santos[2], Lyda Patricia Sabogal-Paz[1], Luiz Antonio Daniel[1]

[1]Department of Hydraulics and Sanitation, São Carlos School of Engineering, University of São Paulo, Av. Trabalhador São-Carlense, 400, 13566-59, São Carlos – São Paulo, Brazil.

[2]Laboratory of Chemical Residues, University of São Paulo, Ribeirão Preto - São Paulo, Brazil.

*Corresponding author.
Tel: +55 43 3315-6102
e-mail address: luanleite@usp.br

Highlights

- Oxidative processes were tested for AOM degradation.
- Highest removal was 29.8 and 67.0% for H_2O_2/Fe(II) and H_2O_2/Fe(II)/UV, respectively.
- High pH values decreased the AOM removal for Fenton and photo-Fenton processes.
- H_2O_2 decay was efficiently fitted in zero model order (R^2>0.95).
- Significant THMFP reduction was found at optimal conditions (42.0 to 83.4%).

GRAPHICAL ABSTRACT

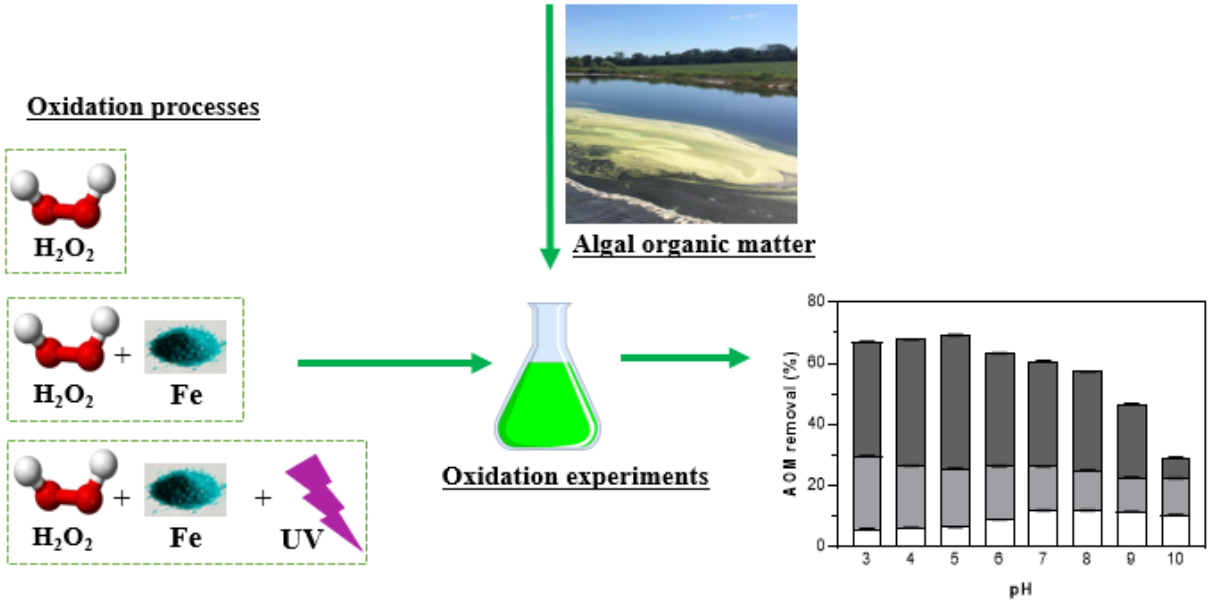

ABSTRACT

Algal organic matter (AOM) in water reservoirs is a worldwide concern for drinking water treatment, once it is one of the main precursors for disinfection by-product formation. Oxidative processes have been widely applied in drinking water treatment to improve microalgae removal, however, there is little information about their performance for AOM degradation. In this context, this study aimed to evaluate the performance of hydrogen peroxide (H_2O_2), Fenton (H_2O_2/Fe(II)), and photo-Fenton (H_2O_2/Fe(II)/UV) processes for AOM removal. Low AOM removals (0.46 to 12.02%) were found using H_2O_2. The highest AOM removals for H_2O_2/Fe(II) (29.8%) and H_2O_2/Fe(II)/UV (67.0%) were obtained using 40 and 30 mg $Fe{\cdot}L^{-1}$ at 150 min, respectively. In general, high pH values decreased AOM removals for H_2O_2/Fe(II) and H_2O_2/Fe(II)/UV processes and increased them for H_2O_2 application. All oxidative processes had stabilized at 150 min and further reaction time did not significantly increase the AOM removal. Trihalomethanes formation potential (THMFP) was evaluated using the optimal conditions of each process. Reductions of THMFP were 42.0, 74.0, and 83.4% for H_2O_2, H_2O_2/Fe(II), and H_2O_2/Fe(II)/UV, respectively. This study showed the potential of oxidative processes to complement AOM removal by the traditional technologies applied in water treatment. Further studies are required to optimize the parameters involved in the process to improve the cost-effectiveness of the processes and applicability in water treatment.

Keywords: AOM, natural organic matter, oxidation process, trihalomethane potential formation; water treatment.

1. INTRODUCTION

The frequent occurrence of algal bloom in drinking water supplies has posed serious problems in drinking water treatment. During algae growth, algal organic matter (AOM), which comprises mainly carbohydrates and proteins, is released by the metabolic processes or cell lysis (Henderson et al., 2008; Naceradska et al., 2019). The AOM presence has a strong impact in the drinking water quality, once it is a well-known precursor of regulated disinfection by-products (trihalomethanes and haloacetic acids) with carcinogenic potential (Goslan et al., 2017; Li et al., 2020; Park et al., 2021). In this context, investigations to improve AOM removal are therefore highly relevant.

Traditional clarification processes (*e.g.*, sedimentation and flotation) applied in water treatment show low/moderate efficiencies for AOM removal. AOM reduction by dissolved air flotation ranges from 46 to 71% using aluminum sulfate (Henderson et al., 2010), while an interval from 25 to 57% is observed for sedimentation using ferric sulfate or polyaluminium chloride (Baresova et al., 2017; Naceradska et al., 2019). Considering the efficiencies shown by these processes, safer water treatment methods are required to remove residual AOM before chlorination to prevent the formation of disinfection by-products (Leite et al., 2022, 2021).

In light of this, oxidation processes are gaining importance to control disinfection by-product formation in water treatment (Kralles et al., 2020; Popov et al., 2020). The H_2O_2/Fe(II) and H_2O_2/Fe(II)/UV processes, known as Fenton and photo-Fenton, respectively, are the most widely used advanced oxidation processes and involve the decomposition of hydrogen peroxide (H_2O_2) catalyzed by a ferrous ion to produce the hydroxyl radicals ($HO^{\bullet}$) (Tsai et al., 2008; Vasquez-Medrano et al., 2018). Dosage of Fenton reagent (H_2O_2 and Fe(II)) and UV dose are the main variables to be considered in the design process and they directly impact the overall efficiency and the total cost (Silva et al., 2016).

H_2O_2/Fe(II) and H_2O_2/Fe(II)/UV processes have been widely applied for natural organic matter degradation (raw water or commercial humic acid). Dissolved organic matter (DOC) removal ranging from 10 to 96% for H_2O_2/Fe(II) and from 10 to 88% for H_2O_2/Fe(II)/UV were

reported using different operational conditions (pH, concentration of H_2O_2 and Fe(II), and UV radiation) (Goslan et al., 2006; Jin et al., 2013; Katsumata et al., 2008; Kitis, 2004; Murray and Parsons, 2004; Wu et al., 2010). These processes are also extensively used as a feasible strategy for improving *Microcystis aeruginosa* removal (Jia et al., 2018; Zhang et al., 2020). However, cyanobacterium organic matter (COM) released from cyanobacteria cells during the oxidative process hampers the determination of COM reduction. This trend in applications highlights the importance of studies analysing only the AOM or COM during the oxidative processes (Micheletto et al., 2020; Shahi et al., 2021). Furthermore, to our knowledge, no specific information is available in the scientific literature regarding the degradation of AOM from green microalgae (such as *Chlorella*), even though this genus is predominant in several algal blooms (Rieper, 1976; Zhang et al., 2010).

In this context, this study investigated the removal of AOM from *Chlorella sorokiniana* by H_2O_2, H_2O_2/Fe(II), and H_2O_2/Fe(II)/UV processes. The main objectives of this paper were: (1) to check the effect of operational variables (H_2O_2/AOM ratio, Fe(II) dosage, and pH values) on the AOM removal; (2) to evaluate the kinetics of AOM degradation and H_2O_2 decay; and (3) to assess the test water quality after the oxidative process treatment using the optimal conditions.

2. MATERIAL AND METHODS

2.1 *Chlorella sorokiniana* cultivation

Chlorella sorokiniana 211-8 k (Culture Collection of Algae and Protozoa, Argyll, Scotland) was used as a strain model in this study. Batch cultivation was carried out in 2.5 L glass bottles at environment temperature (29 ± 1 °C), under continuous illumination with an incident light intensity of 86 $\mu E \cdot m^{-2} \cdot s^{-1}$ and feeding of air enriched with 1.5 % CO_2 ($v \cdot v^{-1}$) at 180 $L \cdot h^{-1}$ per bottle. Each bottle contained 1.8 L of M8a medium, with the following initial concentration ($mg \cdot L^{-1}$): 1800 $(NH_2)_2CO$, 840 $NaHCO_3$, 740 $KH_2 \cdot PO_4$, 260 $Na_2HPO_4 \cdot 2\ H_2O$, 400 $MgSO_4 \cdot 7\ H_2O$, 13 $CaCl_2 \cdot 7\ H_2O$, 116 $C_{10}H_{12}O_8N_2NaFe \cdot 3\ H_2O$, 37.2 $C_{10}H_{14}N_2Na_2O_8 \cdot 2\ H_2O$, 0.062 H_3BO_3, 12.98 $MnCl_2 \cdot 4\ H_2O$, 3.2 $ZnSO_4 \cdot 7\ H_2O$, and 1.83 $CuSO_4 \cdot 5\ H_2O$.

2.2 Cell harvesting and AOM extraction

After 7 days of cultivation, the biomass was centrifuged (1500×*g*, 10 min) and washed twice with ultrapure water to remove metabolites and residues of the culture medium. Then, the biomass was maintained at -20°C until the lysis protocol was carried out.

The protocol of AOM extraction from *Chlorella sorokiniana* cells was performed according to Leite et al. (2019). The centrifuged biomass was suspended in ultrapure water and disrupted using an ultrasonic homogenizer (UP400S, Branson, USA) in batch ice at 75% amplitude of ultrasonication (400 W) and pulse mode of 5 min. The samples were frozen at −20 °C, removed from a freezer, and after reaching the environment temperature, the ultrasonication process was applied again. Then, the material was centrifuged (1500×*g*, 10 min) and the supernatant was filtered using a 0.45 μm membrane filter (GF-5, Macherey-Nagel, Germany) to remove the residual solids. The concentrated AOM was stored at -20 °C until its use.

The AOM was characterized by the dissolved organic carbon (DOC) measured using a Total organic carbon (TOC) analyzer (Shimadzu, Japan). AOM concentration used in the oxidation test was expressed based on DOC value.

2.3 Oxidation experiments

The performance of H_2O_2, H_2O_2/Fe(II), and H_2O_2/Fe(II)/UV processes for AOM degradation was assessed. Solutions of hydrogen peroxide ($H_2O_2 \geq 35\%$ ($w \cdot w^{-1}$), Sigma-Aldrich, Germany) and ferrous sulfate heptahydrate (Fe(II), Sigma-Aldrich, Germany) were prepared in ultrapure water to be used in the tests.

The experiments were carried out in test water (TW) prepared in ultrapure water with 5 $mg \cdot L^{-1}$ of AOM, 25 mg $CaCO_3 \cdot L^{-1}$ of total alkalinity (utilizing 8.5 g $Na_2HCO_3 \cdot L^{-1}$ solution), and pH 8. These values represent the quality usually found in the environment (Leite et al., 2021; Naceradska et al., 2019). The experimental design was divided into three steps, as follows:

(1) H_2O_2 experiments - Response surface methodology was applied to quantify the effect of mass ratio of H_2O_2/AOM (MR, 2 to 42) and reaction time (RT, 30 to 150 min) on the AOM degradation. The analysis was carried out using two factors (Table 1) and optimized using a central composite design, based on a three-factor level (-1, 0, +1) design with face-centered alpha (a=1). The experimental data were analysed by multiple regression and ANOVA using the Minitab software (version 18.1, Minitab LLC., PA, USA). The optimal H_2O_2/AOM MR which reached the highest efficiency was selected and tested in the following steps.

Table 1. Independent variables and their actual values for oxidation test using H_2O_2.

Variables	Units	-1	0	1
MR	-	2	22	42
RT	min	30	90	150

(2) H_2O_2/Fe(II), and H_2O_2/Fe(II)/UV experiments – The tests were carried out with different Fe(II) concentrations (10 to 100 mg $Fe \cdot L^{-1}$) to find the optimal value for each oxidative process. Both processes were performed using 400 mL TW at pH 3, which is the optimum pH value for H_2O_2/Fe(II) and H_2O_2/Fe(II)/UV processes (Goslan et al., 2006). The H_2O_2/Fe(II) tests were performed in 500 mL bottles wrapped with aluminum foil to protect the solutions from light. The H_2O_2/Fe(II)/UV tests were performed in a collimated device with one low-pressure mercury

UV lamp (maximum 15 W, emitting light at 254 nm wavelength) used to deliver the UV dose to the sample. The 400 mL TW was placed in a 1-L beaker resulting in a water layer of 3 cm. The power density of the UV dose used in this study was measured as 0.658 $mW \cdot cm^{-2}$. It represents a UV dose of 1.18, 3.55, and 5.92 $Ws \cdot cm^{-2}$ for the RT of 30, 90, and 150 min, respectively. The UV lamp was turned on for 15 min to reach the maximum intensity before the tests. In the experiments, the appropriate Fe(II) concentration was added to the TW followed by the H_2O_2 solution. Then, the samples were continuously mixed using a magnetic stirrer at 100 rpm and samples were collected at three RTs (30, 90, and 150 min) for characterization in terms of DOC. The optimal Fe(II) concentration of each process that reached the highest efficiency was selected and tested in the following step.

(3) pH effect on these processes - The optimal conditions (MR and Fe(II) concentration) found for each oxidation process were tested in a wide pH range (pH 3 to 10) at three RTs (30, 90, and 150 min). The pH of TW was modified by adding 1N HCl or 1N NaOH (Qhemis, Brazil) before the addition of iron and H_2O_2 solution.

At the end of each test, sodium metabisulfite solution (SMBS, Synth, Brazil) was added to the solution at an SMBS/H_2O_2 mass ratio of 3:1 to neutralize residual H_2O_2 before DOC analysis. Furthermore, samples were collected without the SMBS addition to quantify the residual H_2O_2, soluble iron concentration, and pH. AOM removal from TW in different testing conditions was calculated according to Leite et al. (2021).

.

2.4 Kinetics and H_2O_2 decay modeling

The optimal conditions found for H_2O_2, H_2O_2/Fe(II), and H_2O_2/Fe(II)/UV processes for AOM degradation were performed at different RTs (30 to 390 min). The tests were carried out using TW (5 mg·L^{-1} of AOM, 25 mg $CaCO_3$·L^{-1} of total alkalinity) at pH 8. Samples were collected at appropriate times to be characterized by DOC and residual H_2O_2.

The H_2O_2 decay in each oxidative process was modeled using a zero-order mathematical model (Equation 1) (Falsanisi et al., 2006):

$$C_t = (C_o - D) - k_o t \quad (1)$$

Where C_o and C_t (mg·L^{-1}) are the initial H_2O_2 concentration (210 mg·L^{-1}) and the concentration at time *t* (min), respectively. D (mg·L^{-1}) is the initial oxidant demand and k_o (mg·L^{-1}·min^{-1}) is the first order constant of the model.

Non-linear regression was applied to evaluate the adjustment of the experimental data to the mathematical model (Equation 1) using the Microsoft Office® Excel Solver. To verify model fitting, the predicted and experimental data were analyzed by the coefficient of determination (R^2), the residual root mean square error (RMSE), and the reduced chi-square (χ^2) according to Leite et al. (2018).

2.5 TW quality

The TW quality after the oxidative process treatment was evaluated using the optimal conditions (H_2O_2/AOM MR and Fe(II) dosage) found in previous tests. The tests were done using TW (5 mg·L^{-1} of AOM, 25 mg $CaCO_3$·L^{-1} of total alkalinity, pH 8) and an RT of 150 min. At the end of the test, samples were collected to be characterized by physico-chemical parameters. Total soluble iron, residual H_2O_2, and pH were immediately analyzed, while protein, carbohydrate, and total carbon were quantified after the SMBS addition.

H_2O_2 concentration was determined in presence of phenanthroline using the Spectroquant® Hydrogen Peroxide test (Merck, Germany) at 445 nm. Total iron was quantified by USEPA FerroVer® Method using the Iron Reagent Powder Pillows (Hach, USA) at 510 nm. Protein was measured using the Bradford reagent (Sigma-Aldrich, USA) at 595 nm using bovine serum albumin (Sigma-Aldrich, USA) as standard. Total carbohydrates were determined using the phenol-sulfuric acid method (Dubois et al., 1956) at 488 nm using glucose (Qhemis, Brazil) as standard. Each analysis was done in triplicate.

The potential formation of THM (THMFP) after initial TW and after each treatment was also evaluated. Samples were prepared according to the quality found in the test (pH, alkalinity, and AOM concentration). Chlorination tests were done in 20 mL samples and NaOCl (Sigma-Aldrich, USA) was added at a Cl_2:DOC mass ratio of 5:1. Amber glass bottles were sealed and left in the dark at a temperature of 20 °C for 7 days. After this contact time, free chlorine was quenched with ascorbic acid (Qhemis, Brazil) at a mass ratio of 6:1. Then, the samples were immediately extracted using MTBE as a solvent (Sigma-Aldrich, USA). The THM concentration was quantified using gas chromatography spectrometry (CG-2010 Shimadzu, Japan) using the standard USEPA 551 method (U.S. EPA., 1995). Each condition was performed in duplicates.

2.6 Statistical analyses

Results were expressed as a mean value ± standard deviation. The significance, as well as differences among treatment results, were evaluated using a two-way ANOVA analysis followed by the Tukey test. Statistical analyses were performed using GraphPad Prism software (version 6.01, USA) with a significance level of 0.05.

3. RESULTS AND DISCUSSION

3.1 H_2O_2

The effect of MR (2, 22, and 42) and RT (30, 90, and 150 min) on the AOM degradation is shown in Table 2. Low AOM removals were found in the H_2O_2 experiments ranging from 0.46 to 12.02%. The highest AOM removal (12.02%) was obtained using MR of 42 and RT of 150 min, whereas the lowest removal (0.46%) was found using MR of 2 and RT of 30 min. H_2O_2 showed a low capacity for AOM oxidation which can be observed by low oxidant consumption during the reaction (Table 1). For instance, only 12.9 mg $H_2O_2 \cdot L^{-1}$ was consumed in the best condition (MR of 42 and RT of 150 min) from the 210 mg $H_2O_2 \cdot L^{-1}$ initially added in this test.

Table 2 – Experimental results for the central composite design of AOM removal by H_2O_2.

Condition	MR	RT (min)	AOM Removal (%)	Residual H_2O_2 ($mg \cdot L^{-1}$)
1	2	30	0.46	7.0
2	2	90	0.80	6.8
3	2	150	1.78	6.5
4	22	30	8.33	103.5
5	22	90	9.49	102.2
6	22	150	9.62	101.5
7	42	30	10.11	199.8
8	42	90	11.78	198.6
9	**42**	**150**	**12.02**	**197.1**

A second-degree polynomial function was generated by multiple regression analysis for the data presented in Table 1. ANOVA analysis showed that the quadratic model was highly significant (F-value=587.69, $p < 0.001$), and the lack of fit were statistically insignificant ($p > 0.05$) for the experimental data. A good correlation between experimental ($R^2 = 0.997$) and predicted values (Adj. $R^2 = 0.9959$) was observed. The second-degree polynomial equation generated demonstrated the significance ($p < 0.05$) of both linear (MR and RT) and quadratic (MR^2) factors in predicting the AOM oxidation by H_2O_2. Meanwhile, the interactive (MR×RT)

and quadratic (RT^2) terms were statistically insignificant ($p > 0.05$). Therefore, the final function for AOM degradation by H_2O_2, expressed in terms of actual values, is shown in Equation 2.

$$\text{AOM removal (\%)} = -1.610 + 0.5815 \times MR + 0.02813 \times RT - 0.5815 \times (MR)^2 \quad (2)$$

The low AOM removals (0.46 to 12.02%) observed in the experiments can be explained by the oxidation mechanism and properties of H_2O_2. Although H_2O_2 has a high oxidation potential of 1.37 V, it is a weak oxidant for organic compounds. The H_2O_2 mechanism for organic compound oxidation is the transfer of an electrophilic single oxygen atom from H_2O_2 to an electron-rich site on the compound (Kim and Huang, 2021). However, in the presence of other electrophilic compounds, the H_2O_2 can react as a nucleophile and undergo substitution reactions (a functional group is replaced by another functional group), without showing oxidizing properties during the process (Krupinska, 2020).

It should be noted, however, that the results found in this research are a little higher than other studies about dissolved natural organic matter (NOM) oxidation by H_2O_2. Jin et al. (2013) did not find an apparent humic acid removal using H_2O_2 concentrations lower than 60 $mg \cdot L^{-1}$. In contrast, high H_2O_2 concentrations (50–1000 $mg \cdot L^{-1}$) provided low DOC reductions (less than 7%) in samples from a drinking water reservoir in Turkey (Kitis and Kaplan, 2007). These differences are may associate with the complexity of the water matrices used in each study.

Despite its low potential for the standalone application for AOM oxidation, H_2O_2 has a high capacity for combining with other agents (catalysts or radiation) to lead to the formation of hydroxyl radicals (·OH), which are very strong and nonspecific oxidants (Tsai et al., 2008). Considering this, the performance of H_2O_2/Fe(II) and H_2O_2/Fe(II)/UV processes were also evaluated for AOM degradation. Based on the previous results, the optimal condition (MR of 42, displayed in bold in Table 2) was used in the following steps. A high H_2O_2 concentration was used to hydrogen peroxide not be a limiting reagent in the reactions during the iron variation and the kinetics tests due to H_2O_2 decay in H_2O_2/Fe(II)/UV process.

3.2 H_2O_2/Fe(II) and H_2O_2/Fe(II)/UV

The H_2O_2/Fe(II) process results for AOM degradation using different Fe(II) concentrations are shown in Figure 1a. The presence of Fe(II) significantly increased AOM removal (Tukey test, $p < 0.05$). For instance, AOM removal increased from 6.0 to 21.0 % at 150 min, when 10 mg Fe·L^{-1} was added in the test. The RT showed a significant effect on the AOM removal and |significant differences were observed between the results found at 30 and 150 min (Tukey test, $p < 0.05$). Furthermore, the highest AOM removal (29.8%) was obtained using 40 mg Fe·L^{-1} and RT of 150 min.

Figure 1 – Performance of (a) Fe(II)/UV and (b) H_2O_2/Fe(II)/UV with different Fe(II) concentrations (0 to 100 mg Fe·L^{-1}) and reaction times (30, 90, and 150 min) at pH 3. The tests were carried out using an AOM concentration of 5 mg·L^{-1} and MR of 42.

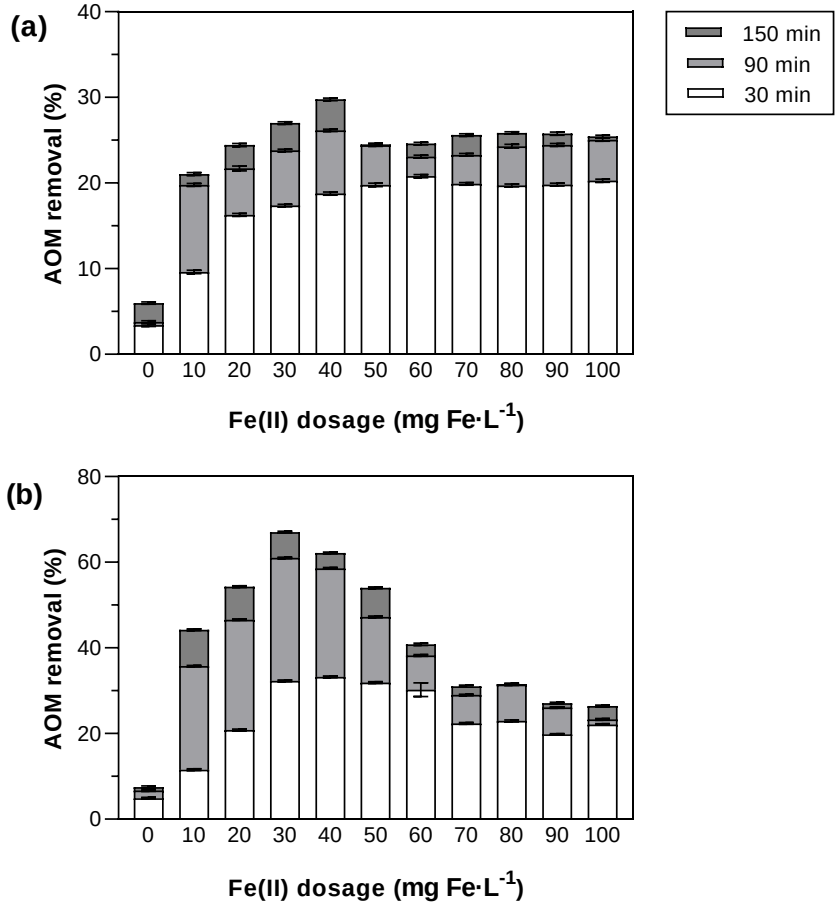

The Fe(II) dosing showed two different trends in AOM removal by H_2O_2/Fe(II) process. The AOM removal increased until the concentration of 40 mg Fe·L^{-1} and decreased when higher Fe(II) concentrations (>40 mg Fe·L^{-1}) were added. AOM removals were 29.8 and 25.4% for 40 and 100 mg Fe·L^{-1}, respectively. Compared to similar research, the same behavior was observed for humic acid oxidation by Fenton (Wu et al., 2010). According to the authors, this happened because the high Fe(II) concentration favored the occurrence of scavenging reaction in the chain termination. Based on these results, the optimal Fe(II) concentration found was 40 mg Fe·L^{-1}.

The effect of different Fe(II) concentrations on the H_2O_2/Fe(II)/UV performance for AOM degradation was also analysed (Figure 1b). Adding Fe(II) significantly increased AOM removal (Tukey test, $p < 0.05$). For example, the AOM removal increased from 7.5 to 44.3% at 150 min, when 10 mg Fe·L^{-1} was added to the test. The RT also led to a significant effect on AOM degradation and significant differences were observed between results found at 30 and 150 min (Tukey test, $p < 0.05$). Additionally, the highest AOM removal (67.0%) was obtained using 30 mg Fe·L^{-1} and an RT of 150 min.

As also observed in the Fenton experiments, the increase in Fe(II) concentration showed two different trends in AOM removal by photo-Fenton. AOM removal increased until the concentration of 30 mg Fe·L^{-1} and decreased the degradation when higher Fe(II) concentrations (>30 mg Fe·L^{-1}) were dosed. The AOM removals were 67.0 and 26.4% for 30 and 100 mg Fe·L^{-1}. The negative effect of a high concentration of Fe(II) was also observed for humic acid degradation using photo-Fenton (Katsumata et al., 2008). Based on the results, the optimal Fe(II) dosage was 30 mg Fe·L^{-1}.

These results are in agreement with previous studies about natural organic matter degradation (raw water or synthetic matrices based on commercial humic acid) by H_2O_2/Fe(II) and H_2O_2/Fe(II)/UV processes. DOC removals from 10 to 96% for H_2O_2/Fe(II) and from 10 to 88% for H_2O_2/Fe(II)/UV were observed using different operational conditions (pH, concentration of H_2O_2 and Fe(II), and UV radiation) (Goslan et al., 2006; Jin et al., 2013; Katsumata et al., 2008;

Kitis, 2004; Murray and Parsons, 2004; Wu et al., 2010). The high range reported makes clear that the water composition plays a significant role in the oxidative process efficiency.

As previously mentioned, H_2O_2/Fe(II) and H_2O_2/Fe(II)/UV have also been applied for cyanobacteria removal, and it includes cyanobacterium organic matter (COM). Zhang et al. (2020) used H_2O_2/Fe(II) to remove *Microcystis aeruginosa* cells and found high efficiencies for COM removal (> 70%). The authors concluded that Fe(III) can destabilize the COM and coagulate cells to settle them down simultaneously. However, the release of COM during the test and the presence of microalgae cells (Jia et al., 2018) hinder an appropriate comparison between the present data and these COM results from peer literature. Besides that, our results for AOM removal were higher than those obtained by studies targeting COM from *Microcystis aeruginosa*. Micheletto et al. (2020) reported the DOC removal ranging from 9.4 to 29.4 % using solar H_2O_2/Fe(II)/UV, while Shahi et al. (2021) found low extracellular COM removals (2 to 5.9 %) using UV/H_2O_2, UV/ClO_2, and UV/Cl_2 processes. These differences are may be associated with the source of organic matter (*e.g.*, type of microorganism, composition, etc.) and the water matrices used in the tests (*e.g.*, culture medium, ultrapure water, etc.)

H_2O_2, H_2O_2/Fe(II), and H_2O_2/Fe(II)/UV processes were tested in a wide pH range (pH 3 to 10) and the obtained results are shown in Figure 2. pH had a significant effect on the performance of such processes (Tukey test, $p < 0.05$) In general, high pH values decreased the AOM removal for H_2O_2/Fe(II) and H_2O_2/Fe(II)/UV processes and increased for hydrogen peroxide application.

Low AOM removals (6.0 to 12.0%) were found for H_2O_2 tests varying from 6.0% at pH 3 to 10.5% at pH 10. At high pH, the H_2O_2 decomposition is catalyzed by the hydroxyl radicals ($OH^{\bullet}$) forming the hydroperoxyl radical ($HO_2^{\bullet}$), which is a strong nucleophile and can oxide organic compounds (Clayton et al., 2011). It may explain the increase in AOM removal at high pH values.

The efficiency observed for the H_2O_2/Fe(II) process decreased from 29.7% at pH 3 to 22.5% at pH 10, while the decay found for H_2O_2/Fe(II)/UV process was more drastic from 67.0 %

at pH 3 to 29.3% at pH 10. Both decreases in performance are associated with the iron form present in the solution, as well as H_2O_2 decay during the reactions. The H_2O_2/Fe(II) and H_2O_2/Fe(II)/UV processes have their maximum catalytic activity at pH 3.0, after which their efficiencies decrease due to the degradation of H_2O_2 into O_2 and H_2O and the precipitation of soluble iron as $Fe(OH)_3$ (Vasquez-Medrano et al., 2018). The higher pH effect on H_2O_2/Fe(II)/UV compared to H_2O_2/Fe(II) process may be due to the higher H_2O_2 decomposition during the test, which is demonstrated in section 3.3. This pH effect on H_2O_2/Fe(II) and H_2O_2/Fe(II)/UV processes is in agreement with a previous study (Murray and Parsons, 2004).

Figure 2 – Performance of H_2O_2, H_2O_2/Fe(II), and H_2O_2/Fe(II)/UV at different pH values (pH 3 to 10) at 150 min. Tests were carried out using an AOM concentration of 5 mg·L^{-1} and the optimal conditions (MR of 42, 40 mg Fe·L^{-1} for H_2O_2/Fe(II), and 30 mg Fe·L^{-1} for H_2O_2/Fe(II)/UV).

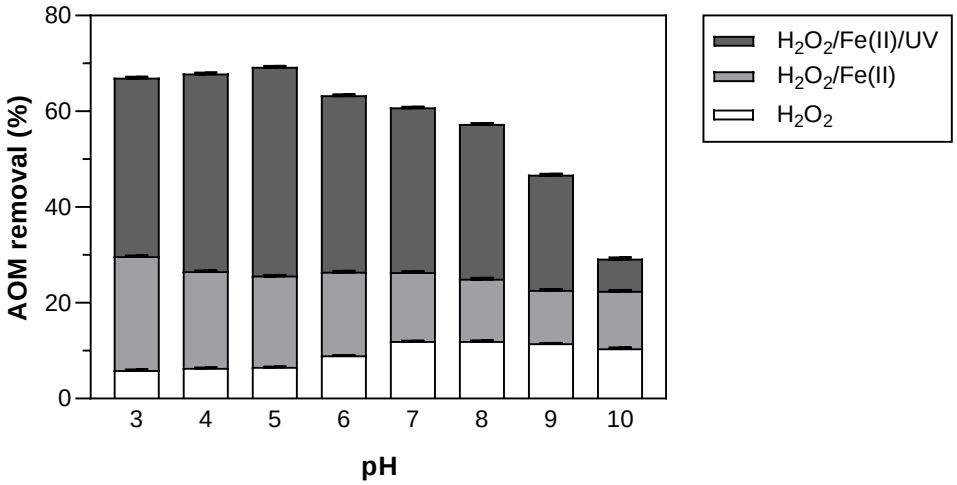

3.3 Kinetics and H_2O_2 decay modeling

AOM oxidation kinetics and H_2O_2 decay at different reaction times were analyzed (Figure 3) under environmental conditions (AOM concentration of 5 mg·L^{-1}and pH 8). All oxidative processes had stabilized at 150 min and further reaction time did not significantly increase AOM removal (Figure 3a). Residual AOM ratio (C/C_0) at 150 min was 0.88, 0.74, and 0.43 for H_2O_2, H_2O_2/Fe(II), H_2O_2/Fe(II)/UV, respectively.

The results showed a low oxidant demand followed by a slow decline decay for H_2O_2, H_2O_2/Fe(II), and a strong decrease for H_2O_2/Fe(II)/UV (Figure 3b). After 390 minutes, considerable residual H_2O_2 was still available in the solution. At the end of the tests, residual H_2O_2 of 196.3, 140.5, and 20.4 mg·L^{-1} were observed for H_2O_2, H_2O_2/Fe(II), and H_2O_2/Fe(II)/UV, respectively. The behavior of hydrogen peroxide decay in H_2O_2/Fe(II)/UV experiments happens due to UV radiation, which can also decompose H_2O_2 into H_2O, HO•, and O (Hunt and Taube, 1952).

Figure 3 – Variation of residual (a) AOM and (b) H_2O_2 for the application of H_2O_2, H_2O_2/Fe(II), and H_2O_2/Fe(II)/UV processes at different reaction times. Predicted values using the zero-order mathematical model are shown in the dashed line. The tests were carried out using an AOM concentration of 5 mg·L^{-1} at pH 8 and the optimal conditions (MR of 42, 40 mg Fe·L^{-1} for H_2O_2/Fe(II), and 30 mg Fe·L^{-1} for H_2O_2/Fe(II)/UV).

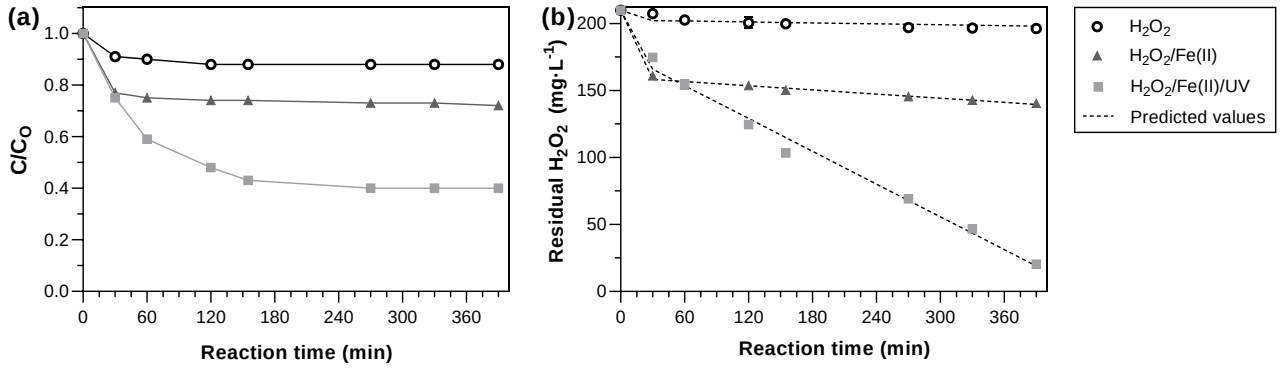

Considering modeling can be an important tool to optimize the residual concentration and improve the cost-effectiveness of these oxidative processes, fitting the experimental data to the zero-order mathematical model (Equation 2) was evaluated. The goodness of fit was analyzed by the coefficient of determination (R^2), residual root mean square error (RMSE), and reduced chi-square ($\chi 2$). The parameter results found by the non-linear regression and the statistical analysis are shown in Table 3. Great adjustments were found to the zero-order model, which is demonstrated by high R^2 (>0.95) values and low $\chi 2$ (<49.6), and RMSE (<5.95) values (Leite et

al., 2018). Therefore, these models can be used to optimize the H_2O_2 dose used and improve the cost-effectiveness of these processes. Although the fact that the zero-order model is used frequently to model the PAA decay (Falsanisi et al., 2006) which contains H_2O_2 in the commercial solution, it had not yet been used for H_2O_2 decay individually.

Table 3 - Results of model fitting parameter for H_2O_2 decay.

Process	k_o (mg·L^{-1}·min^{-1})	D (mg·L^{-1})	R^2	χ^2	RMSE
H_2O_2	0.01132	7.4	0.967	8.72	2.50
H_2O_2/Fe	0.05203	50.1	0.957	2.76	1.40
H_2O_2/Fe/UV	0.40811	31.9	0.987	49.60	5.95

3.4 TW quality

TW quality after the oxidative process treatment was assessed using the optimal conditions found in previous experiments (Table 4). The oxidative processes significantly modified TW quality (Tukey test, $p < 0.05$). The efficiencies of AOM removal in environmental conditions were 12.0, 25.4, and 53.4 % for H_2O_2, H_2O_2/Fe(II), and H_2O_2/Fe(II)/UV processes, respectively.

AOM removal may be also observed by the removal of its main compounds (protein and carbohydrate). Protein removals were 33.5, 37.5, and 57.9 % for H_2O_2, H_2O_2/Fe(II), and H_2O_2/Fe(II)/UV, respectively. As for carbohydrate removals, H_2O_2, H_2O_2/Fe(II), and H_2O_2/Fe(II)/UV led to 8.8, 40.9, and 60.6%, respectively. As can be observed, similar removals of protein and carbohydrate were obtained in H_2O_2/Fe(II) and H_2O_2/Fe(II)/UV.

pH decreased after the oxidative processes and the pH values of 7.4, 3.2, and 3.2 were observed for H_2O_2, H_2O_2/Fe(II), and H_2O_2/Fe(II)/UV experiments, respectively. It might happen due to the H^+ formation in the solution by the addition of ferrous sulfate heptahydrate as a Fe(II) source, which consumes the alkalinity initially added in the TW. This observation is confirmed by the decay of dissolved total carbon content due to inorganic carbon consumption. For instance,

the inorganic carbon (total carbon - AOM) removal was 0.0, 70.6, and 96.1% for hydrogen peroxide, Fenton, and photo-Fenton processes, respectively.

The potential formation of THM was also evaluated (Table 4). The THM present in the samples was chloroform, once the bromide was not present in the AOM. THMFP reduction found was 42.0, 74.0, and 83.4% for H_2O_2, H_2O_2/Fe(II), and H_2O_2/Fe(II)/UV, respectively. It is important to mention that low pH values found in the H_2O_2/Fe(II) and H_2O_2/Fe(II)/UV experiments favor the THMFP formation (Goslan et al., 2006).

Table 4. Comparison between the TW quality found after the oxidation treatment of H_2O_2, H_2O_2/Fe(II), and H_2O_2/Fe(II)/UV processes. Tests were carried out using an AOM concentration of 5 mg·L^{-1} at pH 8 and the optimal conditions (H_2O_2/AOM ratio of 42, 40 mg Fe·L^{-1} for H_2O_2/Fe(II), and 30 mg Fe·L^{-1} for H_2O_2/Fe(II)/UV). Average removals are shown between parentheses.

Parameters	**TW**	**Oxidation processes**		
		H_2O_2	**H_2O_2/Fe(II)**	**H_2O_2/Fe(II)/UV**
AOM (mg·L^{-1})	5.0 ± 0.0	4.4 ± 0.2 (12.0)	3.7 ± 0.3 (25.4)	2.3 ± 0.1 (53.6)
Total carbon (mg·L^{-1})	10.1 ± 0.1	6.7 ± 0.0 (33.5)	5.2 ± 0.0 (48.5)	2.5 ± 0.0 (75.2)
Protein (mg·L^{-1})	2.4± 0.4	1.6 ± 0.1 (33.5)	1.5 ± 0.1 (37.5)	1.0 ± 0.0 (57.9)
Carbohydrates (mg·L^{-1})	5.5± 0.4	5.1 ± 0.7 (8.8)	3.3 ± 0.5 (40.9)	2.2 ± 0.1 (60.6)
pH	8.0 ± 0.0	7.4 ± 0.0	3.2 ± 0.0	3.2 ± 0.0
Dissolved iron (mg Fe·L^{-1})	-	-	16.1 ± 1.3	14.6 ± 1.1
Residual H_2O_2 (mg·L^{-1})	-	199.8 ± 0.4	150.3 ± 0.5	103.4 ± 1.7
THMFP (µg·L^{-1})	311.6 ± 5.0	180.6 ± 0.4 (42.0)	81.0 ± 0.7 (74.0)	51.8 ± 1.1 (83.4)

These results showed the potential of applying H_2O_2/Fe(II) and H_2O_2/Fe(II)/UV processes coupled with other technologies for AOM degradation. However, high residuals of H_2O_2 and Fe were still present in the solution, as displayed in Table 3. The residual H_2O_2 were 199.8, 150.3, and 103.4 mg·L^{-1} for H_2O_2, H_2O_2/Fe(II), and H_2O_2/Fe(II)/UV processes, respectively.

Considering that the costs associated with Fenton reagent (iron and H_2O_2) and UV system are the major issue for the use of this process at full-scale (Silva et al., 2016; Vasquez-Medrano et al., 2018), further studies are required to optimize the parameters involved (UV dose, H_2O_2, and iron concentration). That is encouraged to obtain better cost-effectiveness of the processes and the applicability in water treatment.

4. CONCLUSIONS

This study investigated the removal of AOM from *Chlorella sorokiniana* by H_2O_2, H_2O_2/Fe(II), and H_2O_2/Fe(II)/UV processes. Low AOM removals (0.46 to 12.02%) were found using H_2O_2. The highest AOM removals for H_2O_2/Fe(II) (29.8%) and H_2O_2/Fe(II)/UV (67.0%) were obtained using 40 and 30 mg $Fe \cdot L^{-1}$ at 150 min, respectively. In general, high pH values decreased AOM removal for H_2O_2/Fe(II) and H_2O_2/Fe(II)/UV processes and increased it when H_2O_2.was applied. All oxidative processes stabilized at 150 min and further contact time did not significantly increase AOM removal. THMFP reductions in the optimal condition were 42.0, 74.0, and 83.4% for H_2O_2, H_2O_2/Fe(II), and H_2O_2/Fe(II)/UV, respectively. Overall, this study elucidated the potential of oxidative processes to complement AOM removal by the traditional technologies applied in water treatment. Further research is recommended to assess detailed cost-effectiveness of these processes and provide a framework for implementation in specific contamination scenarios

Acknowledgements

The São Paulo Research Foundation (FAPESP – Proc. 2019/05759-1) granted Luan de Souza Leite with a PhD scholarship. The Coordination for the Improvement of Higher Education Personnel (CAPES-PROEX – Financial code 001) granted Kamila Jessie Sammarro Silva with a PhD scholarship.

Data Availability

The data that support the findings of this study are available from the corresponding author upon reasonable request.

Author contribution

Luan de Souza Leite: Conceptualization; Methodology; Investigation; Formal analysis; Writing – original draft; Writing – review & editing. **Kamila Jessie Sammaro Silva**: Conceptualization; Investigation; Formal, Writing – review & editing. **Danilo Vitorino dos Santos**: Investigation; Formal analysis; Writing – review & editing. **Lyda Patricia Sabogal-Paz**: Supervision; Writing – review & editing. **Luiz Antonio Daniel**: Supervision; Conceptualization; Writing – review & editing.

Declaration of Competing Interest

The authors declare that they have no known competing financial interests or personal relationships that could have appeared to influence the work reported in this paper

References

Baresova, M., Pivokonsky, M., Novotna, K., Naceradska, J., Branyik, T., 2017. An application of cellular organic matter to coagulation of cyanobacterial cells (Merismopedia tenuissima). Water Res. 122, 70–77. https://doi.org/10.1016/j.watres.2017.05.070

Clayton, W.S., Petri, B.G., Huling, S.G., 2011. Fundamentals of ISCO Using hydrogen peroxide, in: Siegrist, R.L., Crimi, M., Simpkin, T.J. (Eds.), In Situ Chemical Oxidation for Groundwater Remediation. Springer, New York, NY, pp. 193–232. https://doi.org/10.1007/978-1-4419-7826-4_5

Dubois, M., Gilles, K.A., Hamilton, J.K., Rebers, P.A., Smith, F., 1956. Colorimetric method for determination of sugars and related substances. Anal. Chem. 28, 350–356. https://doi.org/10.1021/ac60111a017

Falsanisi, D., Gehr, R., Santoro, D., Dell'Erba, A., Notarnicola, M., Liberti, L., 2006. Kinetics of PAA demand and its implications on disinfection of wastewaters. Water Qual. Res. J. Canada 41, 398–409. https://doi.org/10.2166/wqrj.2006.043

Goslan, E.H., Gurses, F., Banks, J., Parsons, S.A., 2006. An investigation into reservoir NOM reduction by UV photolysis and advanced oxidation processes. Chemosphere 65, 1113–1119. https://doi.org/10.1016/j.chemosphere.2006.04.041

Goslan, E.H., Seigle, C., Purcell, D., Henderson, R., Parsons, S.A., Jefferson, B., Judd, S.J., 2017. Carbonaceous and nitrogenous disinfection by-product formation from algal organic matter. Chemosphere 170, 1–9. https://doi.org/10.1016/j.chemosphere.2016.11.148

Henderson, R.K., Baker, A., Parsons, S.A., Jefferson, B., 2008. Characterisation of algogenic organic matter extracted from cyanobacteria, green algae and diatoms. Water Res. 42, 3435–3445. https://doi.org/10.1016/j.watres.2007.10.032

Henderson, R.K., Parsons, S.A., Jefferson, B., 2010. The impact of differing cell and algogenic organic matter (AOM) characteristics on the coagulation and flotation of algae. Water Res. 44, 3617–3624. https://doi.org/10.1016/j.watres.2010.04.016

Hunt, J.P., Taube, H., 1952. The Photochemical Decomposition of Hydrogen Peroxide. Quantum Yields, Tracer and Fractionation Effects. J. Am. Chem. Soc. 74, 5999–6002. https://doi.org/10.1021/ja01143a052

Jia, P., Zhou, Y., Zhang, X., Zhang, Y., Dai, R., 2018. Cyanobacterium removal and control of algal organic matter (AOM) release by UV/H2O2 pre-oxidation enhanced Fe(II) coagulation. Water Res. 131, 122–130. https://doi.org/10.1016/j.watres.2017.12.020

Jin, P., Jin, X., Wang, X., Bai, F., 2013. Effect of ozonation and hydrogen peroxide oxidation on the structure of humic acids and their removal. Adv. Mater. Res. 610–613, 1256–1259. https://doi.org/10.4028/www.scientific.net/AMR.610-613.1256

Katsumata, H., Sada, M., Kaneco, S., Suzuki, T., Ohta, K., Yobiko, Y., 2008. Humic acid degradation in aqueous solution by the photo-Fenton process. Chem. Eng. J. 137, 225–230. https://doi.org/10.1016/j.cej.2007.04.019

Kim, J., Huang, C.-H., 2021. Reactivity of Peracetic Acid with Organic Compounds: A Critical Review. ACS ES&T Water 1, 15–33. https://doi.org/10.1021/acsestwater.0c00029

Kitis, M., 2004. Disinfection of wastewater with peracetic acid : a review. Environ. Int. 30, 47–55. https://doi.org/10.1016/S0160-4120(03)00147-8

Kitis, M., Kaplan, S.S., 2007. Advanced oxidation of natural organic matter using hydrogen peroxide and iron-coated pumice particles. Chemosphere 68, 1846–1853.

https://doi.org/10.1016/j.chemosphere.2007.03.027

Kralles, Z.T., Ikuma, K., Dai, N., 2020. Assessing disinfection byproduct risks for algal impacted surface waters and the effects of peracetic acid pre-oxidation. Environ. Sci. Water Res. Technol. 6, 2365–2381. https://doi.org/10.1039/d0ew00237b

Krupinska, I., 2020. Impact of the oxidant type on the efficiency of the oxidation and removal of iron compounds from groundwater containing humic substances. Molecules 25, 3380. https://doi.org/10.3390/molecules25153380

Leite, L. de S., Daniel, L.A., Pivokonsky, M., Novotna, K., Branyikova, I., Branyik, T., 2019. Interference of model wastewater components with flocculation of Chlorella sorokiniana induced by calcium phosphate precipitates. Bioresour. Technol. 286, 121352. https://doi.org/10.1016/j.biortech.2019.121352

Leite, L. de S., Hoffmann, M.T., de Vicente, F.S., dos Santos, D.V., Daniel, L.A., 2021. Adsorption of algal organic matter on activated carbons from alternative sources: Influence of physico-chemical parameters. J. Water Process Eng. 44, 102435. https://doi.org/10.1016/j.jwpe.2021.102435

Leite, L. de S., Hoffmann, T., de Vicente, F.S., dos Santos, D.V., Mesquita, A., Juliato, F.B., Daniel, L.A., 2022. Screening of new adsorbents to remove algal organic matter from aqueous solutions : kinetic analyses and reduction of disinfection by - products formation. Environ. Sci. Pollut. Res. 1–13. https://doi.org/10.1007/s11356-022-22412-2

Leite, L.D.S., Matsumoto, T., Albertin, L.L., 2018. Mathematical modeling of thermal drying of facultative pond sludge. J. Environ. Eng. 144, 04018079. https://doi.org/10.1061/(ASCE)EE.1943-7870.0001427.

Li, X., Rao, N.R.H., Linge, K.L., Joll, C.A., Khan, S., Henderson, R.K., 2020. Formation of algal-derived nitrogenous disinfection by-products during chlorination and chloramination. Water Res. 183, 116047. https://doi.org/10.1016/j.watres.2020.116047

Micheletto, J., Torres, M.D.A., De Carvalho S. De Paula, V., Cerutti, V.E., Pagioro, T.A., Cass, Q.B., Martins, L.R.R., De Liz, M.V., Martins De Freitas, A., 2020. The solar photo-Fenton process at neutral pH applied to microcystin-LR degradation: Fe2+, H2O2and reaction matrix effects. Photochem. Photobiol. Sci. 19, 1078–1087. https://doi.org/10.1039/d0pp00050g

Murray, C.A., Parsons, S.A., 2004. Removal of NOM from drinking water: Fenton's and photo-Fenton's processes. Chemosphere 54, 1017–1023. https://doi.org/10.1016/j.chemosphere.2003.08.040

Naceradska, J., Novotna, K., Cermakova, L., Cajthaml, T., Pivokonsky, M., 2019. Investigating the coagulation of non-proteinaceous algal organic matter: Optimizing coagulation performance and identification of removal mechanisms. J. Environ. Sci. (China) 79, 25–34. https://doi.org/10.1016/j.jes.2018.09.024

Park, K.Y., Choi, S.Y., Ahn, S. kyung, Kweon, J.H., 2021. Disinfection by-product formation potential of algogenic organic matter from Microcystis aeruginosa: Effects of growth phases and powdered activated carbon adsorption. J. Hazard. Mater. 408, 124864. https://doi.org/10.1016/j.jhazmat.2020.124864

Popov, M., Kragulj Isakovski, M., Molnar Jazić, J., Tubić, A., Watson, M., Šćiban, M., Agbaba, J., 2020. Fate of natural organic matter and oxidation/disinfection by-products formation at a full-scale drinking water treatment plant. Environ. Technol. (United Kingdom) 1–12. https://doi.org/10.1080/09593330.2020.1732474

Rieper, M., 1976. Investigations on the relationships between algal blooms and bacterial

populations in the Schlei Fjord (western Baltic Sea). Helgoländer Wissenschaftliche Meeresuntersuchungen 28, 1–18. https://doi.org/10.1007/BF01610792

Shahi, N.K., Maeng, M., Choi, I., Dockko, S., 2021. Degradation effect of ultraviolet-induced advanced oxidation of chlorine, chlorine dioxide, and hydrogen peroxide and its impact on coagulation of extracellular organic matter produced by Microcystis aeruginosa. Chemosphere 281, 130765. https://doi.org/10.1016/j.chemosphere.2021.130765

Silva, T.F.C.V., Fonseca, A., Saraiva, I., Boaventura, R.A.R., Vilar, V.J.P., 2016. Scale-up and cost analysis of a photo-Fenton system for sanitary landfill leachate treatment. Chem. Eng. J. 283, 76–88. https://doi.org/10.1016/j.cej.2015.07.063

Tsai, T.T., Kao, C.M., Yeh, T.Y., Lee, M.S., 2008. Chemical oxidation of chlorinated solvents in contaminated groundwater: Review. Pract. Period. Hazardous, Toxic, Radioact. Waste Manag. 12, 116–126. https://doi.org/10.1061/(ASCE)1090-025X(2008)12:2(116)

U.S. EPA., 1995. Method 551.1: Determination of chlorination disinfection byproducts, chlorinated solvents , and halogenated pesticides/ herbicides in drinking water by liquid-liquid extraction and gas chromatography with electron-capture detection, Revision 1.0. Cincinnati, OH.

Vasquez-Medrano, R., Prato-Garcia, D., Vedrenne, M., 2018. Ferrioxalate-Mediated Processes, in: Ameta, S.C., Ameta, R. (Eds.), Advanced Oxidation Processes for Wastewater Treatment: Emerging Green Chemical Technology. Academic Press, pp. 89–113. https://doi.org/10.1016/B978-0-12-810499-6.00004-8

Wu, Y., Zhou, S., Qin, F., Zheng, K., Ye, X., 2010. Modeling the oxidation kinetics of Fenton's process on the degradation of humic acid. J. Hazard. Mater. 179, 533–539. https://doi.org/10.1016/j.jhazmat.2010.03.036

Zhang, J.L., Zheng, B.H., Liu, L.S., Wang, L.P., Huang, M.S., Wu, G.Y., 2010. Seasonal variation of phytoplankton in the DaNing River and its relationships with environmental factors after impounding of the Three Gorges Reservoir: A four-year study. Procedia Environ. Sci. 2, 1479–1490. https://doi.org/10.1016/j.proenv.2010.10.161

Zhang, X., Ma, Y., Tang, T., Xiong, Y., Dai, R., 2020. Removal of cyanobacteria and control of algal organic matter by simultaneous oxidation and coagulation - comparing the H2O2/Fe(II) and H2O2/Fe(III) processes. Sci. Total Environ. 720, 137653. https://doi.org/10.1016/j.scitotenv.2020.137653